SUPPLEMENT TO THE *WELDING JOURNAL,* DECEMBER 2012
Sponsored by the American Welding Society and the Welding Research Council

Development of an Oxyrutile Electrode for Wet Welding

An experimental electrode improved weld metal properties such as diffusible hydrogen, porosity, and ductility when wet welding in shallow waters on structural ship steels

BY V. R. SANTOS, M. J. MONTEIRO, F. C. RIZZO, A. Q. BRACARENSE, E. C. P. PESSOA, R. R. MARINHO, AND L. A. VIEIRA

ABSTRACT

The present paper describes the experimental development of an oxyrutile electrode. The aim of this experimental work was to improve the weld metal mechanical properties and minimize the diffusible hydrogen content compared to existing commercial electrodes. Eighteen batches of electrodes were produced in industrial facilities. Nickel and molybdenum were added to strengthen the weld metal. Most welding trials were carried out using laboratory simulations and also by divers in the sea at 10 m depth, thereby aiming for qualification up to 20 m according to AWS D3.6M:2010. The mechanical properties, chemical composition, porosity, and microstructures of the weld metal among other features are presented. For comparison, three commercial electrodes were also tested. The results and the progress toward achievement of structural Class A welds are discussed. Most of the experimental electrodes had low porosity and very few weld metal microcracks. The diffusible hydrogen content in this work was equivalent to that of typical oxidizing electrodes. Generally, in comparison to the results reported in the literature, the oxyrutile electrodes developed here showed lower porosity and had superior performance in terms of toughness and ductility. Overall, the results represent a significant improvement in the quality of wet welds, and most of them consistently exceeded the requirements for Class A.

Introduction

Considering the growing number of offshore floating production platforms in operation, as well as the economic limitations for dry docking these structures, wet welding by shielded metal arc welding (SMAW) is a very attractive technique for maintenance and structural repairs (Ref. 1). Wet welds are classed as A and B according to AWS D3.6M:2010, *Underwater Welding Code* (Ref. 2). For Class A welds, the requirements of toughness, strength, ductility, hardness, and bending are similar to those required by the main engineering codes for atmospheric welding. There are very few reports in the literature about achieving Class A in wet welding. Class B welds are considered welds with limited structural quality, where both the tests applied for procedure qualification and the acceptance criteria are less strict. The improvement of wet weld quality has been based on the improvement of the commercially available atmospheric welding electrodes that presented the best weldability and operability underwater. Rutile-based electrodes are generally preferred due to their good operability. Commercial electrode evaluations as well as new coating compositions were made by Stalker (Ref. 3), Nóbrega (Ref. 4), Gooch (Refs. 5, 6), West (Ref. 7), Liu (Ref. 8), Ibarra (Ref. 9), and Sanchez-Osio (Ref. 10). The general conclusions of these works can be summarized as follows: Austenitic electrodes are susceptible to solidification cracking and formation of bands of hard martensite along the fusion boundaries; ferritic electrodes have the best performance and are divided into two groups: rutile-based electrodes and iron oxide-based (oxidizing) electrodes. The former have good arc stability and other running characteristics as well as tensile strength and toughness. The oxidizing electrodes have low diffusible hydrogen content (H_{dif}) and poor operability. In general, oxidizing electrodes have a rough bead surface, and the slag is difficult to remove. The main properties of weldments made by rutile- and oxidizing-type electrodes in terms of weld metal properties and weldability are summarized in Table 1.

In the 1970s, Nobrega (Ref. 4) carried out work to develop an electrode with the combined properties of the rutile- and oxidizing-type electrodes. In spite of the good results achieved, no commercial electrode based on this development can be found on the market today.

Due to expectations that the need for underwater structural maintenance on offshore production platforms will grow, the wet welding consumables (WWC) project was launched to develop an oxyrutile electrode for wet welding. The participants in this project are two universities, an oil company, and an electrode manufacturer. The main aim was to develop an electrode based on iron oxide and titanium oxide with improved mechanical properties minimizing the H_{dif}. Also, operability should

KEYWORDS

Underwater Welding
Wet Welding
SMAW
Covered Electrodes
Diffusible Hydrogen
Electrode Development
Oxidizing Electrode
Oxygen

V. R. SANTOS, M. J. MONTEIRO, and F. C. RIZZO are with the Materials Engineering Department, Pontifícia Universidade Católica do Rio de Janeiro, Rio de Janeiro, Brazil. A. Q. BRACARENSE is with the Mechanical Engineering Department, Universidade Federal de Minas Gerais, Belo Horizonte, Brazil. E. C. P. PESSOA is with the Instituto Federal de Educação, Ciência e Tecnologia de Minas Gerais, Betim, Brazil. R. R. MARINHO is with the PETROBRAS Research Center, Rio de Janeiro, Brazil. L. A. VIEIRA is with ESAB Indústria e Comércio Ltda., Contagem, Minas Gerais, Brazil.

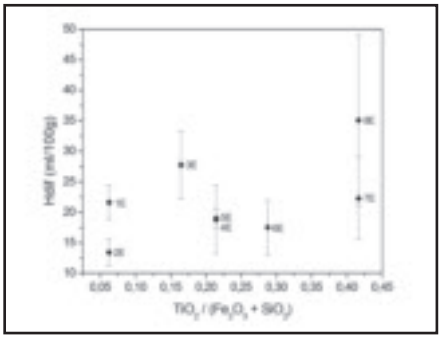

Fig. 1 — Influence of $TiO_2/(Fe_2O_3 + SiO_2)$ in the coating on the diffusible hydrogen (tests at 0.5 m welding depth).

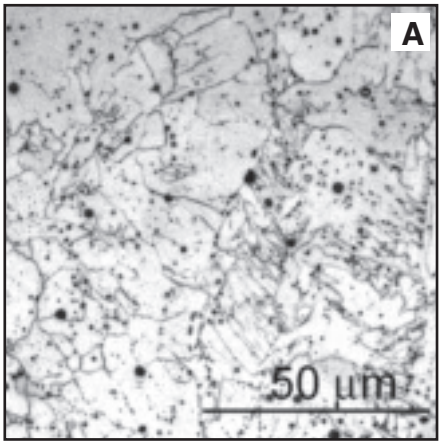

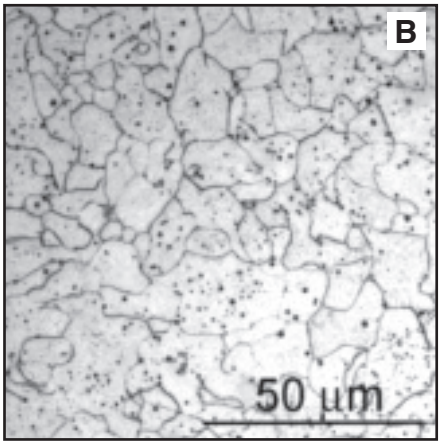

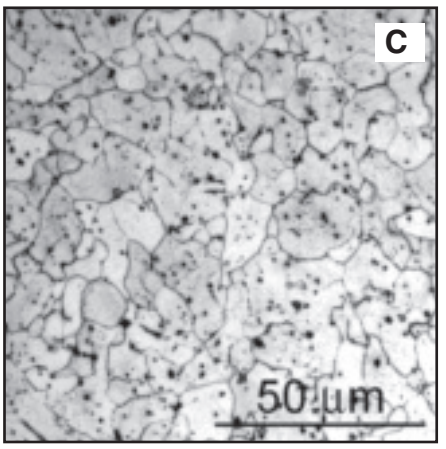

Fig. 2 — Microstructures. A — CR; B — CGR; C — FGR. Representative of experimental electrode (1E to 8E) weld metal microstructures. Nital 2%. Welding depth: 0.5 m.

be improved in relation to the typical oxidizing types. Welding trials were carried out in simulated depths of 10 m in the laboratory and in the open sea, aiming procedures qualification for up to 20 m according to AWS D3.6M:2010. The open sea tests aimed a prequalification of two wet welding procedures, applicable up to 20 m in order to enlarge the options for the repair designer concerning the electrode selection.

The first phase of the WWC project was to select an optimized coating composition as a base line for further developments. The main criteria were to achieve the lowest possible H_{dif}, improve weldability, and maximize the rutile content. The second phase targeted the improvement of weld metal properties with the addition of alloying elements. The improvement of operability was again included in the second phase, but this development step is not presented in this paper. Commercial electrodes were also tested. Results have already been published (Refs. 12, 13).

The aim of the present paper is to describe the development of the WWC project and present selected results emphasizing weld metal mechanical properties and diffusible hydrogen. Other features of the weld metal such as porosity and microstructure are also presented. Comparisons with the state-of-the-art electrodes are made, and the progress toward achievement of structural Class A welds is discussed.

Experimental Methods

Welding tests in Phase 1 of the WWC project were carried out in the laboratory by a mechanized gravity system at 0.5 m water depth. This low depth was chosen in order to guarantee that the experiments could maximize the influences of the base electrode coating composition and minimize the influences of other variables that could be affected by pressure, like presence of pores and weld metal chemical composition. Eight experimental electrode batches were produced for Phase 1. These electrodes were named 1E to 8E according to the increasing rutile content. The coating formulations were based on the combination of hematite (Fe_2O_3) ranging from 40 to 60 wt-%, rutile (TiO_2) ranging from 5 to 25 wt-%, and silica (SiO_2) ranging from 10 to 40 wt-%, which totaled 85

Table 1 — Comparative Properties of Rutile and Oxidizing Type Electrodes Based on Literature Data

	Rutile Electrodes	Oxidizing Electrodes
Weld metal chemical composition (Refs. 11–13)	Increasing depth decreases manganese and silicon and increases oxygen.	Low sensitivity to depth. High oxygen and low manganese and silicon at all depths.
Diffusible hydrogen (Refs. 14–17)	High (< 90 mL/100 g). Decreases with increasing pressure.	Medium (< 20 mL/100 g). As low as 13 mL/100 g has been reported.
Porosity (Refs. 18–23)	Increases considerably with depth	Increases moderately with depth in shallow waters. (<30 m)
Mechanical strength (Refs. 11, 24–28)	Class E 70XX is commonly achieved.	Low-strength deposits. Class E 60XX is commonly achieved.
Ductility (Refs. 12, 26, 28)	Low elongation (< 15%) in the tensile test. Decreases with depth.	Possible to achieve elongation around 20% up to 20 m.
Toughness (Refs. 29, 30)	Commonly meets the requirements of the main standards or codes.	Commonly meets requirements of the main standards or codes.
HAZ hydrogen cracking (Refs. 31, 32)	High cracking susceptibility for C > 0.15% and C.E. > 0.38%.	Low cracking susceptibility for structural steels in general.
WM hydrogen cracking (Refs. 12, 13)	High cracking susceptibility in general.	Low cracking susceptibility in general.

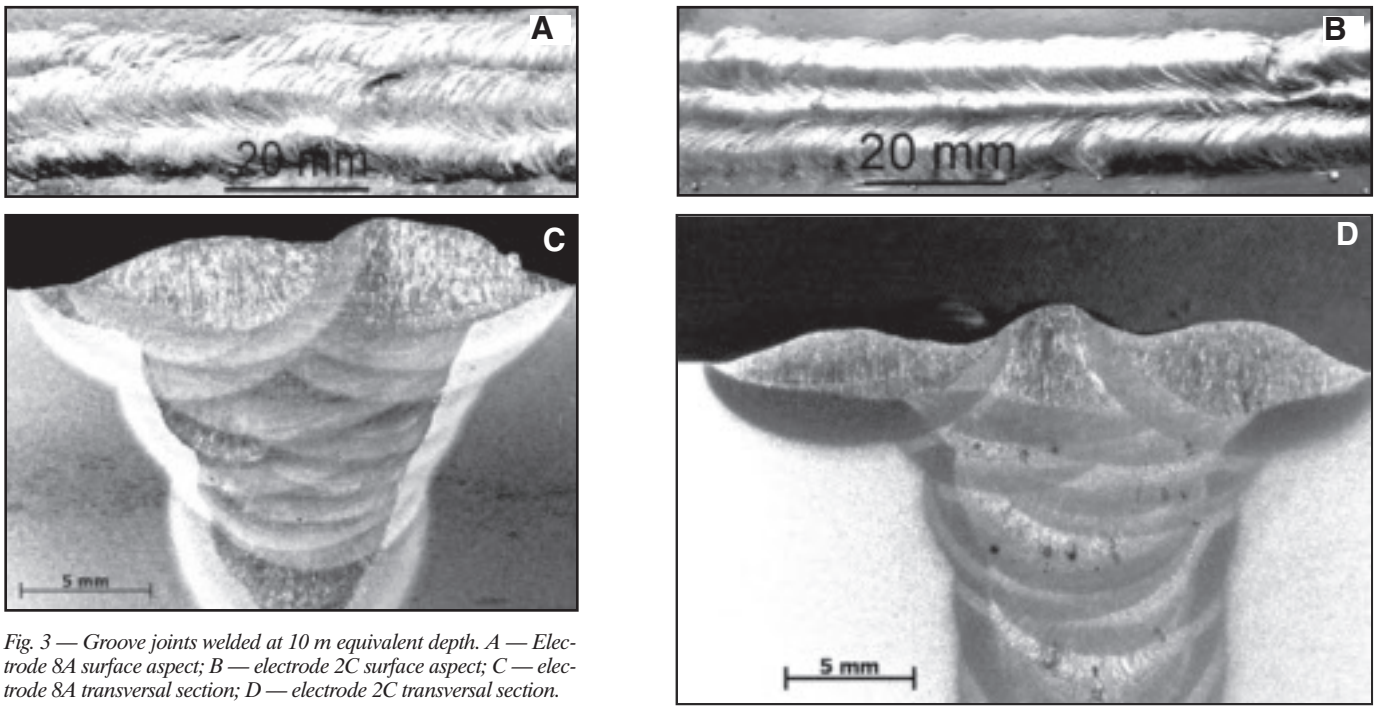

Fig. 3 — Groove joints welded at 10 m equivalent depth. A — Electrode 8A surface aspect; B — electrode 2C surface aspect; C — electrode 8A transversal section; D — electrode 2C transversal section.

wt-%. The remaining 15 wt-% had invariant amounts of binding agents, gases and slag formers, and arc stabilizers. The coating composition of the best electrode in this phase was applied as the base composition for further improvements in Phase 2. In this second phase, Ni and FeMo were added to improve mechanical properties by alloying the weld metal.

In Phase 2, 25 experimental electrode batches were produced. In this phase, the aim was to improve the weld metal properties by adding Ni and Mo and also to improve operability by arc stabilizers and minor additions of exothermic substances. The electrodes named 1A, 2A, and 3A had increasing additions of Ni. The electrodes 5A to 10A had increasing additions of Ni plus Mo. The alloying additions, made by Ni powder and Fe-Mo, never exceeded 3% and the reduction of the other ingredients of the base formulation were proportionally distributed. Therefore, it is assumed that no relevant differences would occur between either the oxiding potential and operational behavior of the electrodes 1A–10A, with the exception for electrode 9A, which received an extra addition of arc stabilizer compounds. The remaining experimental electrodes were those designed to improve operability, and their results do not belong in the scope of this paper. The commercial electrodes tested were named 1C (oxidizing type), and 2C and 3C (rutile type) electrodes. Most of tests in Phase 2 were performed in the laboratory by a mechanized gravity system at pressure equivalent to 10 m water depth. Some manual welding trials were made in the open sea down to 10 m with electrodes 9A and 2C. A few laboratory tests with selected electrodes were

Table 2 — Summary of Welding Conditions According to Depth

Phase	Electrode Code	Laboratory 0.5 m	Laboratory 10 m	Laboratory 20 m	Open sea 10 m
1	1E to 8E	X			
2	1A and 2A	X	X	X	
2	3A, 5A to 8A		X		
2	4A		X	X	
2	9A		X		X
2	10A		X		
Commercial	1C and 3C	X	X	X	
Commercial	2C	X	X	X	X

Table 3 — Electrodes Steel Rod and Base Metal Compositions (wt-%)

		C	Si	Mn	P	S	Cr	Ni	Mo	Cu
Electrodes steel rod	Min spec.	0.04	—	0.40	—	—	—	—	—	—
	Max spec.	0.08	0.02	0.60	0.01	0.015	0.05	0.1	0.05	0.05
	Typical	0.06	0.01	0.47	0.0065	0.011	0.025	0.04	0.004	0.028
Base metal ASTM A36		0.15	0.20	0.85	0.022	0.007	0.023	0.012	—	0.008
Base metal ASTM AH 36		0.16	0.23	1.41	0.016	0.006	0.01	0.01	0.001	0.01

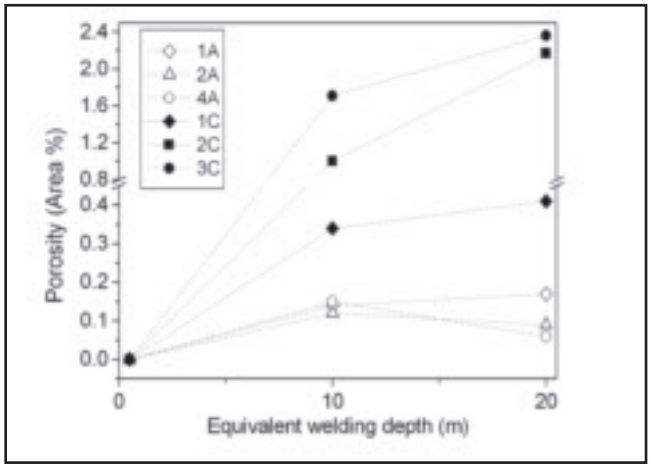

Fig. 4 — Porosity as a function of depth for selected experimental and commercial electrodes.

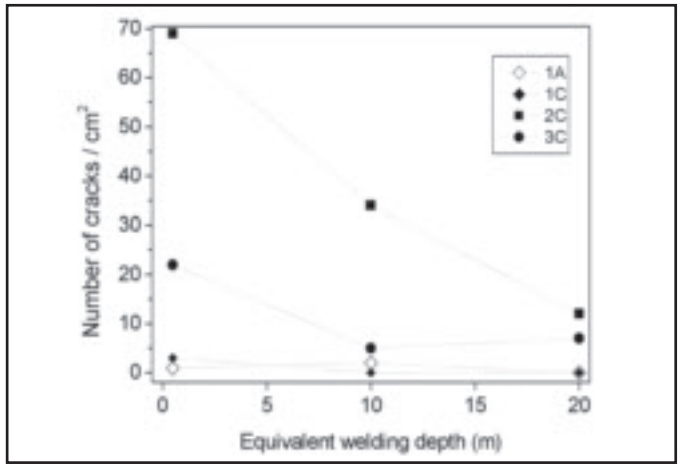

Fig. 5 — Quantitative weld metal transverse crack evaluation in longitudinal sections of groove welds as a function of pressure

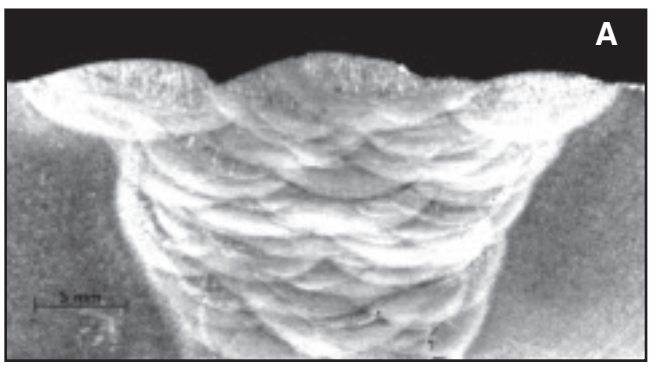

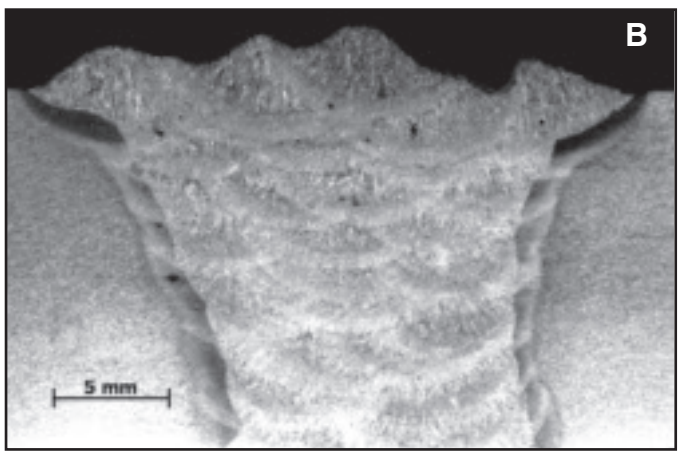

Fig. 6 — Macrographs of groove joints welded at 10 m in open sea. A — Electrode 9A; B — electrode 2C.

performed at 0.5 m water depth and at pressure equivalent to 20 m to evaluate the influence of pressure. The test matrix for the whole project according to the welding depth is presented in Table 2.

All electrodes had 3.25-mm diameters and were 350 mm long. Commercial electrodes 2C and 3C were provided with a waterproof coating; however, the manufacturers did not disclose the composition and application techniques. The electrode 1C and the experimental electrodes were coated by dipping in a vinyl varnish. Electrodes steel rods and base metal compositions are presented in Table 3.

In the laboratory, welding tests were carried out with a welding power source operating on direct current electrode negative (DCEN) at a nominal 160 A. A tank with capacity of 200 L was used for the welds at 0.5 m water depth. A hyperbaric welding simulator was used for the welds of 10 m and 20 m equivalent depth. All the welds were carried out in fresh water with a mechanized gravity system and using the drag technique in the flat position and with an electrode angle of 60 deg. The welding voltage and current were monitored by an acquisition system with a rate of 1000 Hz. The weld beads were deposited in V grooves with an opening angle of 45 deg, root opening of 3.25 mm, and 13.0 mm depth, machined on ASTM A36, 16 × 280 × 150 mm plates.

Qualified AWS D3.6 Class B welders carried out the open sea welding tests. The power source was an electronic constant current characteristic, specially built for wet welding, operating on DCEN at a nominal 160 A. The weld beads were deposited in V grooves with backing, an opening angle of 45 deg, a root opening of 10 mm, and a root face of 3 mm. Base materials were ASTM AH36 16 × 280 × 150 mm plates.

A gas chromatography analyzer carried out the diffusible hydrogen measurements according to AWS A4.3, ASTM E260, and E355. All samples were welded at 0.5 m.

The chemical composition (except oxygen) was defined using optical emission spectrometry. A gas analyzer (LECO) was used for the oxygen content.

Metallographic preparation was carried out by conventional polishing and etching techniques. The quantities of the weld metal columnar region (CR), coarse grain reheated region (CGR), and fine grain reheated region (FGR) were measured under 50× magnification in the cross section, along a 10-mm line, perpendicular to the plate surface, located in the center of the weld. The relative quantities of microconstituents were determined by counting points, applying a grid of 100 points over images with 500× magnification. The grain size in the FGR was determined by the intersection method with 500× magnification.

Energy X-ray dispersive spectroscopy (EDS) was used to determine the chemical composition of at least 6 inclusions with diameters between 4 and 8 μm.

Vickers hardness loads of 1 and 10 kgf were used to measure the weld metal hardness. The all-weld tensile tests were prepared in accordance with AWS D3.6M:1999. The samples were 5 mm in diameter and had a 25-mm gauge length, or dimensions that are indicated in the table footnotes.

In the laboratory welding tests, 5000 voltage and current readings were acquired between the 10th and 15th second. The following parameters were calculated: average current (I_{ave}), average voltage (V_{ave}), current arc stability index (S_i), volt-

age arc stability index (S_v), and indicative number of short circuits (N_{sc}). The parameter S_i is defined as the ratio of maximum to minimum values of current. Similarly, for voltage, the values of S_v are defined as the ratio of maximum to minimum values of voltage. The following approach was used to calculate the values of S: for each 10 points (0.01 second), values of current were taken and the maximum current (I_{max}) was divided by the minimum current (I_{min}) obtaining 500 values of S for each weld. With these values, the average S was calculated. A short circuit was assumed when any voltage value was numerically lower than 5 V.

Geometrical bead reinforcement (R/W) and penetration (P/W) aspect ratios related to the bead width (W) were measured on transverse sections of the bead on plate trials.

Results

Phase 1 – Electrodes 1E to 8E (Tests at 0.5 m)

Diffusible Hydrogen. The results of diffusible hydrogen measurements at 0.5 m for the experimental electrodes (1E to 8E) are listed in Table 4. For comparison, results for commercial electrodes are presented in the same table: typical rutile (2C and 3C) and oxidizing (1C) electrodes. Diffusible hydrogen values from the experimental electrodes are much lower than the rutile electrodes and near to the oxidizing electrode values. The influence of the coating rutile content on the diffusible hydrogen for the experimental electrodes is shown in Fig. 1. As the $TiO_2/(Fe_2O_3 + SiO_2)$ ratio increases, there is a tendency for the diffusible hydrogen to increase.

Weld Metal Chemical Composition

Table 5 lists the results of the weld metal chemical composition for experimental electrodes and, for comparison, commercial electrodes. Despite the variations of rutile and iron oxide contents, there was not a significant change in the weld metal chemical composition for the experimental electrodes. The low contents of Mn and Si, which are deoxidizer elements, are characteristic of oxidizing-type electrodes (Refs. 3–6, 12, 13). Rutile electrodes 2C and 3C had higher Si and Mn contents compared to the high oxygen potential electrode 1C and the experimental electrodes. Electrodes 2C and 3C had consistently lower oxygen contents in the weld metal.

Microstructural Aspects

The quantitative results of microstructural characterization for the experimental electrodes (1E to 8E) are listed in Table 6. The columnar region is formed predominantly by proeutectoid ferrite for all electrodes. Some regions of polygonal ferrite and side plate ferrite can also be observed. This fact is a consequence of the low carbon, manganese, and silicon contents, which are characteristic of oxidizing-type electrodes. No significant microstructural differences were observed between the experimental

Table 4 — Diffusible Hydrogen Measured from Samples Welded at 0.5 m Water Depth (mL/100 g)

Electrode	Sample 1	Sample 2	Sample 3	Sample 4	Sample 5	Average
1E	21.0	24.7	19.2	—	—	21.6
2E	13.3	15.7	11.3	—	—	13.4
3E	25.6	34.3	33.1	23.3	22.7	27.8
4E	26.8	13.6	17.3	17.6		18.8
5E	17.4	19.4	20.3	—	—	19.0
6E	16.6	13.4	16.2	23.9	—	17.5
7E	15.4	21.4	28.1	16.3	30.3	22.3
8E	40.4	56.2	20.9	25.2	32.7	35.1
1C	18.7	24.5	18.1	—	—	20.4
2C	85.1	105.2	78.9	72.3	—	85.4
3C	98.8	101.4	91.4	—	—	97.2

Table 5 — Weld Metal Chemical Composition (wt-%)

Electrode	Mn	Si	P	S	C	O	Ni
1E	0.041	0.013	0.016	0.010	0.012	0.270	0.019
2E	0.041	0.012	0.015	0.008	0.022	0.242	0.021
3E	0.046	0.014	0.016	0.008	0.015	0.310	0.112
4E	0.072	0.070	0.019	0.009	0.016	0.320	0.029
5E	0.047	0.008	0.023	0.008	0.019	0.267	0.019
6E	0.049	0.015	0.021	0.031	0.011	0.255	0.024
7E	0.064	0.034	0.036	0.014	0.013	0.264	0.025
8E	0.044	0.009	0.025	0.007	0.014	0.276	0.019
1C	0.033	0.010	0.015	0.007	0.055	0.261	2.020
2C	0.513	0.384	0.014	0.009	0.070	0.092	0.069
3C	0.343	0.199	0.026	0.007	0.090	0.11	0.026

(a) Welding depth: 0.5 m.

Table 6 — Quantitative Microstructural Characterization

Electrode	PEF + PF + SPF in the CR (%)	CR (%)[b]	CGR (%)[b]	FGR (%)[b]	FGS (μm)	
					Average	St. Dev
1E	100	25	13	62	8.0	1.8
2E	100	37	10	53	8.8	1.9
3E	100	27	9	64	7.3	1.5
4E	100	31	10	59	8.3	1.7
5E	100	26	9	65	6.9	1.4
6E	100	27	16	57	10.2	2.2
7E	100	38	10	52	7.3	1.1
8E	100	37	15	48	5.6	1.1

CR: columnar region. CGR: coarse-grain region in reheated zone. FGR: fine-grain region in reheated zone. PEF: pro-eutectoid ferrite. PF: polygonal ferrite. SPF: side plate ferrite. FGS: grain diameter in FGR.
(a) Welding depth: 0.5 m.
(b) Average for 3 transversal sections.

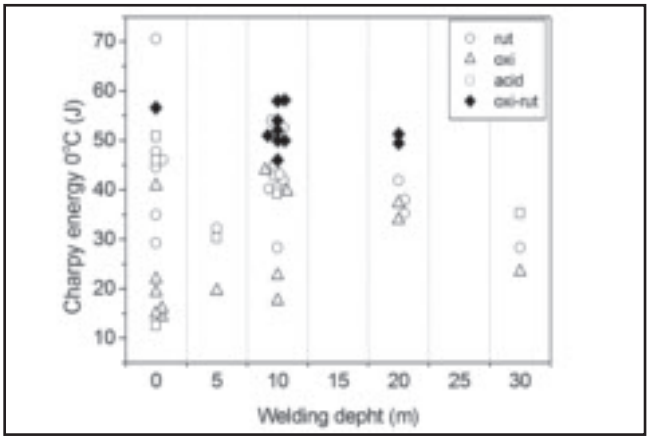

Fig. 7 — Charpy results of oxyrutile electrodes compared with the ones available in the technical literature (Refs. 1, 3, 4, 6, 7, 12, 27, 28, 33, 36, 38–41, 43). Oxyrutile data for 10 and 20 m are from WWC project.

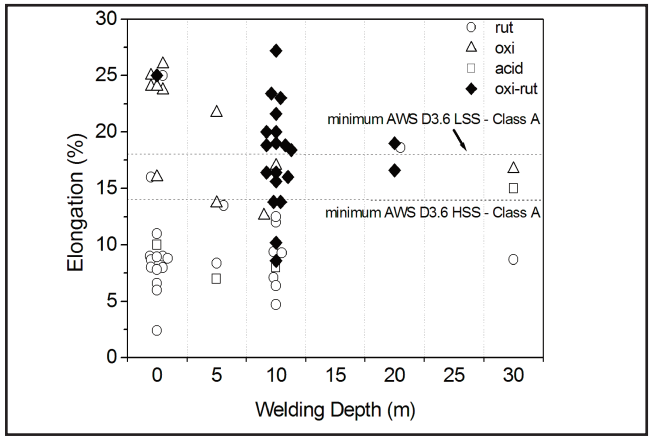

Fig. 8 — Elongation results of oxyrutile electrodes compared with the ones available in the technical literature (Refs. 1, 3, 4, 7, 12, 27, 28, 33, 36, 38–43). Oxyrutile data for 10 and 20 m are from WWC project. Minimum requirements for high-strength steels (HSS) and low-strength steels (LSS) are represented by dashed lines.

electrodes. The exception is the variation of the grain size in the fine-grain region, which may be attributed to variations in welding parameters and conditions. Representative images of the microstructures are shown in Fig. 2. A large amount of nonmetallic inclusions can be observed. The fine-grain region corresponds to the major part of the weld metal for all experimental electrodes.

Mechanical Properties

The average hardness and Charpy values are listed in Table 7. The low hardness and toughness values are typical of oxidizing-type electrodes. No consistent influence of rutile contents on hardness could be noticed. Toughness seems to be slightly increased with increasing rutile content. These results are in agreement with microstructural analysis, which shows a nonsignificant influence of rutile content in the microstructure. The small variation of toughness may be attributed to a small decrease of the grain size in the FGR with increasing rutile content.

Analysis of Nonmetallic Inclusions

The results of EDS analysis are summarized in Table 8. For comparison, the results of the commercial electrodes are also tabulated. Two groups of electrodes can be identified. The group represented by the commercial rutile electrodes 2C and 3C has high Mn, Si, and Ti and low Fe contents according to the lower oxidizing potential of these electrodes. The group represented by the experimental and commercial 1C electrodes has high Fe and almost no Ti, indicating high oxidizing potential during welding. The additions of rutile did not induce a measurable effect on the composition of the inclusions, since it was not possible to identify significant differences between the results of electrodes 1E to 8E.

Table 7 — Weld Metal Hardness and Toughness

	Hardness (HV1)		Charpy V 0°C (J)	
Electrode	Average	St. Dev.	Average	St. Dev.
1E	174	5	22.6	3.3
2E	152	2	15.0	1.5
3E	180	10	30.4	7.7
4E	153	2	21.3	6.3
5E	162	6	27.1	10.0
6E	148	4	22.6	5.1
7E	152	1	25.5	4.3
8E	179	7	37.3	6.8

(a) Welding depth: 0.5 m.

Table 8 — Chemical Composition of Inclusions in the Weld Metal for Experimental and Commercial Electrodes[a] (wt-%)

	Fe		Mn		Si		Ti		O	
Electrode	Average	St. Dev.	Average	St. Dev.	Average	St. Dev.	Average	St. Dev.	Average	St. Dev.
1E	66.3	4.2	3.5	0.9	4.8	2.2	0.0	—	25.5	1.4
2E	65.7	6.6	3.3	1.5	6.3	3.0	0.0	—	25.8	2.0
3E	66.6	3.9	4.6	1.1	3.9	1.9	0.0	—	24.9	1.2
4E	59.9	7.0	6.3	3.3	6.8	2.7	0.0	—	26.9	1.8
5E	54.7	10.0	6.7	1.9	9.7	5.1	0.0	—	28.8	3.3
6E	65.5	6.7	4.6	1.3	4.6	3.3	0.0	—	25.3	2.2
7E	64.7	4.0	5.9	1.9	4.0	1.3	0.0	—	25.0	0.9
8E	59.2	11.1	6.4	3.3	7.3	4.8	0.0	—	27.1	3.2
1C	55.8	7.6	7.3	2.7	8.5	3.1	0.0	—	28.3	2.0
2C	11.8	5.6	24.1	1.5	15.7	4.2	11.9	5.5	36.4	2.3
3C	12.5	5.5	20.7	2.9	20.7	5.5	7.3	2.5	38.3	3.1

(a) Welding depth: 0.5 m.

The main requirement for selecting the best performance electrode in Phase 1 was the diffusible hydrogen content. Therefore, to compare operational features only, the four lowest H_{dif} electrodes were considered. The results are listed in Table 9. Although the electrode 2E (Table 4) had the lowest diffusible hydrogen result (13.4 mL/100 g), the electrode 6E (17.5 mL/100 g) was selected as the basis for Phase 2 based on its better operational performance, as indicated by lower N_{sc} and higher V_{ave} and P/W. The higher rutile content in the coating was also considered an important feature of the electrode 6E. The other weld metal properties (Tables 4 to 8) in general did not show sufficient differences between the experimental electrodes to influence the final choice.

Table 9 — Operability Parameters for the Lowest Diffusible Hydrogen Electrodes

	2E	4E	5E	6E
V_{ave}	22	25	20	27
I_{ave}	161	162	166	160
S_v	2.0	1.6	2.2	1.6
S_i	1.5	1.7	1.4	1.5
N_{sc}/5s	95	36	215	10
R/W	0.18	0.17	0.23	0.16
P/W	0.15	0.18	0.18	0.24

Phase 2 — Electrodes 1A to 10A (Tests at 10 m)

The typical weld metal surface and transverse aspects for experimental oxyrutile electrodes (8A) and for commercial

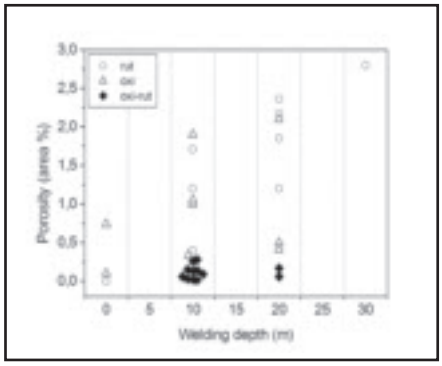

Fig. 9 — Porosity results of oxyrutile electrodes compared with the ones available in the technical literature (Refs. 12, 18, 33, 27, 43). Oxyrutile data are from WWC project.

Table 10 — Weld Metal Properties of V-Grooved Joints Welded in the Laboratory at 10-m Simulated Depth Except for Diffusible Hydrogen Tests, which Samples Were Welded at 0.5 m

Electr.	Y.S. (MPa)[a]	U.T.S. (MPa)[a]	Elong. (%)[a]	Hardness (HV10)[b]		Charpy V 0°C (J)[c]		Side Bend	Porosity (%)	H_{dif} (mL/100 g)[c]	
				Aver.	Min/Max	Aver.	Min/Max	2T[d]		Aver.	Min/Max
1A	398	462	19.0	172	158/180	50	48/51	4/5	0.14	20.9	14.6/30.6
2A	399	464	13.8	155	151/157	58	56/61	4/7	0.13	18.8	15.6/24.0
	399	461	18.4								
3A	407	482	20.0	190	174/220	52	48/54	4/4	0.021	—	—
	417	479	18.8								
4A	421	486	16.4	180	172/190	—	—	5/6	0.15	21.4	14.5/28.7
	427	493	20.00								
5A	410	483	27.2	187	172/206	50	48/52	—	0.09	—	—
6A	437	505	16.4	181	173/186	—	—	1/4	0.03	20.7	16.0/27.7
7A	423	493	15.6	193	172/226	54	52/56	—	0.06	—	—
	441	504	23.4								
8A	412	534	18.8	184	177/190	46	46/46	0/4	0.28	50.0	27.1/71.1
	464	487	8.6								
9A	441	515	16.0	174	171/177	—	—	2/5	0.26	30.8	20.2/53.8
	463	533	21.6								
	440	513	23.0								
10A	434	496	10.2	194	184/218	51	50/54	—	0.014	—	—

(a) All-weld-metal tension tests for each specimen. Lowest elongation values correspond to a higher incidence of weld defects in the tensile specimen.
(b) Average of five indentations minimum.
(c) Average for three specimens minimum. Samples welded at 0.5 m.
(d) Number of approvals/number of tests.

Table 11 — Chemical Composition (wt-%),Amount of Fine Grain Region (area %) and Minimum Grain Size (μm) in the Weld Metal

		Electrode									
		1A	2A	3A	4A	5A	6A	7A	8A	9A	10A
C		0.052	0.024	0.031	0.054	0.034	0.048	0.027	0.037	0.053	0.040
Si		0.009	0.018	0.010	0.014	0.011	0.015	0.022	0.016	0.016	0.019
Mn		0.048	0.048	0.048	0.046	0.047	0.046	0.058	0.049	0.047	0.057
Ni		2.01	1.82	2.70	2.55	1.98	2.55	2.17	2.56	2.37	2.52
Mo		0.00	0.00	0.00	0.05	0.09	0.10	0.125	0.11	0.18	0.20
FGR (area %)		76	87	—	69	81	74	75	—	56	79
FGS (μm)	Average	3.9	3.7	3.7	2.9	3.1	2.8	3.0	—	3.1	3.1
	Std. Dev.	0.7	0.4	0.3	0.3	0.4	0.3	0.3	—	0.4	0.4

P content range: 0.016 to 0.044 wt-%
S content range: 0.008 to 0.015 wt-%
(a) Multipass V-grooved joints welded in laboratory at 10 m simulated depth.

Table 12 — Weld Metal Mechanical Properties of Multipass V Butt Joints[f]

Electrode	Y.S. (MPa)[a]	U.T.S. (MPa)[a]	Elong (%)[a]	Rupture Stress (MPa)[b]	Hardness (HV10)[c]	Charpy V 0°C (J)[d]	Side Bend $2^2/_3T$[e]	Side Bend 6T[e]
9A	488	547	14.4	527/515	221 Min Max 201 229	42.3 Min Max 38 46	2/4	4/4
2C	488	506	6.4	527/494	223 Min Max 194 250	44.0 Min Max 42 47	0/4	4/4

(a) All-weld-metal tension tests for each specimen.
(b) Transversal tensile test.
(c) Average of five indentations minimum.
(d) Average for three specimens minimum.
(e) Number of approvals/number of tests.
(f) Welding at open sea down to 10 m.

Table 13 — Weld Metal Microstructural Characterization on Multipass V Butt Joints[d]

Electr.	Cracks (number per cm^2)	Porosity (%)	Weld metal regions (%)			Weld metal micro-constituents (%)					FGS (μm)	
			CR	CGR	FGR	AF	PEF	FSP	PF	AFC	Aver.	Std. Dev.
9A	0.0	0.09	2	30	68	3.4	2.8	1.0	89.0	3.8	2.3	0.3
2C	62.0	0.32	30	27	43	21.3	22.3	2.8	51.8	1.7	3.0	0.4

CR: Columnar region; CGR: Coarse-grain region; FGR: Fine-grain region; AF: Acicular ferrite;
PEF: Pro-eutectoid ferrite; FSP: Ferrite with second phase; PF: Polygonal ferrite. FGS: Ferritic grain size in the FGR
(a) Welding at open sea down to 10 m.

rutile-type electrodes (2C) are shown in Fig. 3. The weld made with electrode 2C exhibited a superior bead surface and a higher porosity level.

Table 10 lists some selected weld metal properties emphasizing mechanical properties related to the project phases in which the main target was the improvement of strength, ductility, and toughness by adding alloying elements and keeping diffusible hydrogen and porosity at low levels. The ultimate tensile strength (UTS) and elongation results are mostly higher than 490 MPa and 14%, respectively, which are the minimum levels required for AWS D3.6 Class A welds. Hardness and Charpy tests data conformed to the same criteria. The rather unusually low porosity and diffusible hydrogen levels responsible for obtaining elongation values in the order of 20% should be noted. Approval in the bend tests according to the AWS D3.6 Class A criteria were not consistently achieved. Failures occurred from small defects such as pores despite the good weld metal ductility.

The weld metal chemical compositions as well as the main microstructural features responsible for promoting strength, toughness, and ductility are presented in Table 11. High amounts of the fine-grain region can be observed. Small grain size in the reheated zone indicates the beneficial effects of Ni and Mo alloying made in the Phase 2 of the project.

Figure 4 shows the influence of equivalent water depth on porosity for selected electrodes. The experimental electrodes show very little sensitivity to increasing pressure in the range studied.

An evaluation of the incidences of hydrogen cracks in the weld metal as a function of pressure was carried out by manual counting on transversal sections microscopic images. The results are shown in Fig. 5. It is interesting to note the sharp decrease of crack incidences with depth for rutile type electrodes particularly for electrode 3C. The lower crack incidence for electrode 3C compared to electrode 2C in the welding at 10 m was consistent with its lower weld metal hardness (~164 HV10). The value obtained for electrode 2C was ~209 HV10. Moreover, diffusible hydrogen for rutile electrodes is considered to decrease with increasing pressure (Ref. 34). Diffusible hydrogen and hardness are assumed to be the main controlling factors of weld metal cracking in wet welding. As a general tendency in this work, it is pointed out that oxidizing and oxyrutile electrodes showed lower incidence of weld metal microcracks. A survey for weld metal microcracks in all the Phase 2 samples welded at 10 m with oxyrutile electrodes revealed practically no cracks.

Results of Open Sea Tests

Electrodes 2C and 9A were selected for the open sea tests aiming for prequalification of procedures with both types of electrodes for welding high-strength structural ship steels. The electrode 9A was chosen because it produced welds in laboratory with UTS above 513 MPa and good elongation results, reaching reliably the UTS requirement for E70XX class, as shown in Table 10. Tables 12 and 13 list the mechanical properties and microstructural characterization related to the joints welded by divers down to 10 m, respectively. Both electrodes had tensile strength higher than 490 MPa compatible with E70XX class. The commercial electrode 2C had low ductility. The bending test results for both electrodes satisfied the AWS D3.6M:2010 Class B requirements but not the Class A requirements. The fine-grain region was the predominant region for the electrode 9A in both field and laboratory tests. Figure 6 shows macrographs for both electrodes in which lower porosity and smaller amount of columnar regions are related to electrode 9A.

Discussion

Regarding the development of an optimized base composition of an oxyrutile electrode (objective of Phase 1), the tests performed at 0.5-m water depth indicated a composition in which the rutile oxide content was maximized without changing significantly the H_{dif} comparing to a typical oxidizing commercial electrode (both are in the order of 20 mL/100 g). These results are in accordance with results obtained by other authors (Refs. 3–6, 13–17) and accredit oxyrutile electrodes for welding higher carbon equivalent and carbon content steels without hydrogen cracking compared to rutile electrodes. Regardless of the different rutile contents in the coatings of electrodes 1E to 8E, no significant

changes in the weld metal and nonmetallic inclusions in the chemical composition were observed, as well as no observable changes in the microstructural features. Hardness and toughness seemed to show a small increase with rutile content, but the data were limited in extent and may not be statistically significant. However, this was not considered to be an important factor for electrode selection in this phase of the work. As the only powerful strengthening mechanisms for high-oxygen weld metals in wet welding are grain refinement and solid solution, electrode selection criteria were restricted to diffusible hydrogen and operability. In view of these two properties, the electrode 6E was selected as the basis for the composition development in Phase 2.

In terms of improving the mechanical properties, the addition of the alloying elements Ni and Mo to the weld metal was successful for most electrode batches as shown in Table 10. The toughness measured by Charpy energy exceeds the limits required by the AWS D3.6M:2010, *Underwater Welding Code*. The tensile strength results show that it is possible to overcome the lower boundary value of 490 MPa required for class E70XX. Considering the achievement of Class A welds, the ductility results, expressed by elongation and bending, are promising. For the base metal yield strength higher than 350 MPa, the minimum limits for the values of elongation (14%) and bending (180 deg) were mostly achieved. These good results of ductility are associated not only to the high portion of the reheated region and small grain size (Table 11), but also to the low porosity and absence of cracks in the weld metal as shown in Table 10 and Figs. 3–5.

The open sea results shown in Table 13 are useful to point out significant differences between microstructural features for rutile and oxyrutile electrodes tested in this project. In the oxyrutile type, the very low content of acicular ferrite is counterbalanced by the higher proportion of the fine-grain region and polygonal ferrite. According to Table 12, both electrodes tested in the open sea had tensile strength, hardness, and toughness results compatible to electrodes class E70XX and the requirements of AWSD3.6M:2010 Class A. It is well known that especially in wet welding, the properties of the weldments depend strongly on several operational factors, such as welder's skills, sea conditions, visibility, and other factors. The open sea test results were similar to the laboratory test results, suggesting that the properties of the oxyrutile electrodes developed are reproducible and consistent with laboratory results at depths up to 10 m. Nevertheless, considering their limited number, other welding trials at sea are necessary to assure the performance under real conditions of the oxyrutile electrodes developed in this project. For this purpose, more welding trials with divers will soon be performed.

The ductility of the experimental electrode 9A measured by elongation and bending results indicates an enhancement in the achievable quality of wet welding compared to the state of the art. At this stage of the project, the bending test is considered the main barrier to butt joint weld procedure qualifications in AWS D3.6 Class A.

The low ductility, typical of rutile wet weld metal deposits in shallow waters, reported by several authors (Refs. 7, 9, 28, 33) and confirmed in this project, is attributed mainly to the presence of transverse microcracks in the weld metal (Refs. 12, 13). The cracking phenomenon tends to diminish with increasing pressure according to Fig. 5. Two factors may explain this feature: 1) the reduction of the diffusible hydrogen, and 2) the reduction of the weld metal hardness and yield strength caused by the Mn and Si losses. Ando and Asahina (Ref. 34) reported that diffusible hydrogen decreases and porosity increases with increasing pressure and a pore gas composition of almost 100% hydrogen was observed. Consistently, Santos et al. (Ref. 12) reported a decrease in the incidence of HAZ hydrogen cracks with increasing pressure. So, the occurrence of cold cracking both in the weld metal and HAZ seems to be dependent on the porosity. The present results (Figs. 4, 5) suggest that the hydrogen trapping in the pores is the main mechanism responsible for this. The pores can operate as sinks for the hydrogen atoms during their movement to the metal surface and HAZ, thereby reducing the amount of available hydrogen for the cold cracking process.

In order to demonstrate the significance of the present results to the state of art in wet welding, plots of some critical properties (toughness, ductility, and porosity, Figs. 7 to 9, respectively) were made. In these figures, results for the experimental electrodes 1A to 10A are compared to data collected from the literature. Regarding Charpy results, it is well known that toughness has not been a significant problem in wet welding in shallow waters, as confirmed in Fig. 7. In this present literature survey, the commonly adopted minimum of 27 J is exceeded for all rutile and oxyrutile electrodes. Oxidizing and acid electrodes sometimes failed. The results for oxyrutile electrodes were in general the highest and, despite the scattering presented in the results at 10 m, are consistent regarding the possibility of obtaining Class A welds. The lowest result (46 J) is probably related to higher porosity and diffusible hydrogen contents, according to Table 10. Regarding ductility, it is well known that good elongation results constitute the strongest barrier to produce structural quality welds at any depth. In this literature survey, the 14% minimum elongation established by D3.6M:2010 for high-strength steels has not been consistently reported until now — Fig. 8. Also depicted in Fig. 8, three events for rutile electrodes and ten for oxidizing electrodes can be observed above the 14% borderline. Nevertheless, despite the high scattering caused by the presence of defects in some tensile specimens, most of the oxirutile results reported (~80%) exceeded the 14% borderline, demonstrating an increased feasibility of obtaining qualification in Class A. Regarding porosity, the very low values for oxyrutile electrodes seem to be strongly associated to their low diffusible hydrogen content. Regardless of the method used by other authors to measure the porosity, it can be assumed that the results presented in Fig. 9 distinguish the oxyrutile electrodes from the others. It is also important to note the repeatability in the porosity results obtained for oxyrutile electrodes and the high agreement with the results obtained in the open sea tests (Table 13). In summary, toughness, elongation, and porosity results related to oxyrutile electrodes are consistently better compared to the rutile-type electrodes. The most significant progress achieved in this work is the consistent set of elongation results opening up new possibilities for qualification in Class A. Low porosity and absence of microcracks are understood here to be the main features responsible for this breakthrough.

Conclusions

The diffusible hydrogen content of about 20 mL/100 g achieved in the development of oxyrutile electrodes is approximately equivalent to the content of typical oxidizing electrodes and considerably lower than the typical contents of the rutile-type electrodes. Low porosity and the absence of weld metal microcracks were consequently achieved as well as enhanced operability related to the commercial oxidizing electrode.

In Phase 1, all-weld-metal-compositions had low Mn and Si and high oxygen contents as well as iron-rich inclusions. These features are typical of high oxidizing potential electrodes and similar to those observed for the commercial oxidizing electrode tested. The additions of Ni and/or Mo were effective in strengthening the weld metal. Based on the present results, class E70XX electrodes for wet welding can be manufactured. In general, compared to the results obtained in the literature, the electrodes developed here showed lower porosity and presented superior performance in terms of toughness (Charpy energy) and ductility (elongation).

The elongation results represent the most significant contribution of the present work in the search for upgraded weld metal mechanical properties, focusing on wet welding of structural ship steels in shallow waters.

Acknowledgments

The authors wish to express their gratitude to professors Sidnei Paciornick and Marcos Henrique de Pinho Maurício from PUC-Rio for images acquisition and processing; Continental Serviços Marítimos Ltd. for the diving resources in the open sea tests; and the Brazilian Council for Scientific and Technological Development CNPq for graduate scholarships.

References

1. Marinho, M. G., Pope, A. M., Meniconi, L. C., Alves, L. H. M., and Delvechio, C. 2005. Integrity assessment and on-site repair of a floating production platform. *24th International Conference on Offshore Mechanics and Arctic Engineering – OMAE*, paper 67504, Halkidiki, Greece.

2. *Underwater Welding Code*, ANSI/AWS D3.6M:2010, American Welding Society, Doral, Fla.

3. Stalker, A. W. 1977. *Underwater Welding for Offshore Installations*. Welding Institute Research on Underwater Welding. The Welding Institute: 63–74.

4. Nóbrega, A. F. 1981. Study of underwater welding with covered electrodes. MSc dissertation. Federal University of Rio de Janeiro, Brazil (in Portuguese).

5. Gooch, T. G. 1983. Properties of underwater welds. Part 1: Procedural trials. *Metal Construction* (3): 164–167.

6. Gooch, T. G. 1983. Properties of underwater welds. Part 2: Mechanical properties. *Metal Construction* (4): 206–216.

7. West, T. C., Mitchell, G., and Lindberg, E. 1990. Wet welding electrode evaluation for ship repair. *Welding Journal* 69(8): 48.

8. Liu, S., Olson, D. L., and Ibarra, S. 1994. Electrode formulation to reduce weld metal hydrogen and porosity. *Proceedings 13th Offshore Mechanics and Arctic Engineering Conference OMAE*. Copenhagen, Denmark, pp. 291–298.

9. Ibarra, S., Reed, R. L., Smith, J. K., Pachniuk, I., and Grubbs, C. 1991. Underwater wet welding repair of an offshore platform in the North Sea. *Proceedings of the First International Offshore and Polar Engineering Conference*. Edinburgh, UK, pp. 339–346.

10. Sanchez-Osio, A., Liu, S., Ibarra, S., and Olson, D. L. 1995. Designing shielded metal arc consumables for underwater wet welding in offshore applications. *J. Offshore Mech. Arctic Eng*, 117(3): 212–220.

11. Liu, S., Pope, A. M., and Daemen, R. 1994. Welding consumables and weldability. *International Workshop on Underwater Welding of Marine Structures*, La., pp. 321–350.

12. Santos, V. R., Monteiro, M. J., Rizzo, F. C., Bracarense, A. Q., Pessoa, E. C. P., Reppold, R., Domingues, J. R., and Vieira, L. A. 2010. Recent evaluation and development of electrodes for wet welding of structural ship steels. *Proceedings of the 29th International Conference on Ocean, Offshore and Arctic Engineering*. Shanghai, China.

13. Bracarense, A. Q., Pessoa, E. C. P., Santos, V. R., Monteiro, M. J., Rizzo, F. C., Paciornik, S., Reppold, R., Domingues, J. R., and Vieira, L. A. 2008. Comparative study of commercial electrodes for underwater wet welding, *IIW International Congress – 2nd Latin American Welding Congress XXXIV CONSOLDA*, Congresso Nacional de Soldagem, São Paulo, Brazil.

14. Pope, A. M., and Liu, S. 1996. Hydrogen content of underwater wet welds deposited by rutile and oxidizing electrodes. *Proc. Conf. OMAE 96*, American Society of Mechanical Engineers 3: 85–92.

15. Medeiros, R.C., and Liu, S. 1998. A predictive electrochemical model for weld metal hydrogen pickup in underwater wet welds. *ASME Journal of Offshore Mechanics and Arctic Engineering* 120(4): 243–248.

16. Pope, A. M., Medeiros, R. C., and Liu, S. 1995. Solidification of underwater wet welds. *Proceeding Offshore Mechanics and Arctic Engineering Conference*. Copenhagen, Denmark.

17. Pope, A. M. 1995. Oxygen and hydrogen control in shielded metal underwater wet welding, PhD dissertation, Metallurgical and Materials Engineering Department, Colorado School of Mines, Golden, Colo.

18. Suga, Y., and Hasui, A. 1986. On the formation of porosity in underwater weld metal. IIW Doc. IX 1388, 86.

19. Pessoa, E. C. P., Bracarense, A. Q., Liu, S., Guerrero, F. P., and Zica, E. M. 2006. Porosity variation along multipass underwater wet welds and its influence on mechanical properties. *Journal of Materials Processing Technology*, Elsevier, 179: 239–243.

20. Perez, F. 2007. The mechanism of porosity formation in underwater wet welds using SMAW process. PhD dissertation, Colorado School of Mines, Golden, Colo.

21. Pessoa, E. C. P., Bracarense, A. Q., and Liu, S. 2007. Exothermic additions in a tubular covered electrode and oxidizing reactions influence on underwater wet welding. *26th International Conference on Offshore Mechanics and Arctic Engineering,* OMAE.

22. Pessoa, E. C. P., Bracarense, A. Q., and Liu, S. 2008. Estudo do comportamento da porosidade ao longo de soldas subaquáticas molhadas multipasses. *Metalurgia e Materiais* 64: 150–152.

23. Andrade, L. G. D., Silva, W. C. D., Ribeiro, L. F., Pessoa, E. C. P., Bracarense, A. Q., and Liu, S. 2010. The effect of base metal and core rod carbon content on underwater wet weld porosity. *Proceedings of the 29th International Conference on Ocean, Offshore and Arctic Engineering.*

24. Ibarra, S., Olson, D. L., and Grubbs, C. E. 1989. Underwater wet welding of higher strength offshore steels. *21st Annual Offshore Technology Conference,* Paper OTC 5898, Houston, Tex.

25. Kim, M. A. 2003. Study on the development of underwater wet welding electrodes. *Journal of Ocean Engineering and Technology* 17(4): 52–58.

26. Pope, A. M., Liu, S., Teixeira, J. C. G., Santos, V. R., and Paes, M. T. P. 1995. Use of nickel to improve the mechanical properties of high oxygen underwater wet welds, OMAE, *Materials Engineering* 3: 102–117.

27. Santos, V. R., Teixeira, J. C., Piza, M. T. P., and Szelagowski, P. 1992. Final report on project UWT 8, wet welding. German/Brazilian Cooperation in Scientific Research and Technological Development, Rio de Janeiro, Brazil

28. SSC-370. *Underwater Repair Procedures for Ship Hulls*. 1993. Fatigue and Ductility of Underwater Wet Welds Ship Structure Committee.

29. Perez, F., Liu, S., Smith, C., and Rodrigues, E. 2003. Effect of nickel on toughness of underwater wet welds. *Proceeding of OMAE 2003-37291, 22nd International Conference on Offshore Mechanics and Arctic Engineering*, American Society of Mechanical Engineers.

30. Murzin, V., and Russo, V. L. 1994. Manual underwater welding structures of steel with higher strength. *Welding International* 8(1).

31. Ozaki, H., Naiman, J., and Masubuchi, K. 1977. A study of hydrogen cracking in underwater steel welds. *Welding Journal* 56(8): 231-s to 237-s.

32. Kinugawa, J., Fukushima, S., and Fukushima, T. 1982. Influence of equivalent carbon content of steels on proportions of martensite, hardness and susceptibility to cold cracking at coarse-grained regions in underwater wet welding. *Transaction of National Research Institute of Metals* 24(3): 125–133.

33. Rowe, M. D., and Liu, S. 2001. Recent developments in underwater wet welding. *Science and Technology of Welding and Joining* 6(6): 387–396.

34. Ando, S. E., and Asahina, T. 1983. A study on the metallurgical properties of steel welds with underwater gravity welding, *Underwater Welding, IIW Conference*. Trondheim. Pergamun Press, pp. 255–261.

35. Rowe, M. D., Liu, S., and Reynolds, T. J. 2002. The effect of ferro-alloy additions and depth on the quality of underwater wet welds. *Welding Journal* 81(8): 156-s to 166-s.

36. SSC335, Ship Structure Committee, *Performance of Underwater Weldments*, 1990.

37. Szelagowski, P., Pachniuk, I., and Stuhff, H. 1992. Wet welding for platform repair. *Proceedings Second International Offshore and Polar Engineering Conference.* San Francisco, Calif. International Society of Offshore and Polar Engineers (ISOPE), Golden, Colo., pp. 208–215.

38. Grubbs, C., and Reynolds, T. 1998. State-of-the-art underwater welding. *World Oil* (7): 79–83.

39. Grubbs, C., and Reynolds, T. 1999. Underwater wet welding. *Underwater*, Winter, pp. 52–55.

40. Nóbrega, A. F. 1977. Soldagem submarina. *Boletim Técnico da Petrobras* 20(3): 205–219 (in Portuguese).

41. Kim, Min-Nam. 2003. A study on the development of underwater wet welding electrodes. *Journal of Ocean Engineering and Technology* 17(4): 52–58.

42. Silva, E. A., and Hazlett, T. H. 1971. Shielded metal arc welding underwater with iron powder electrodes. *Welding Journal* 50(6): 406.

43. Working Group. 2010. *Underwater Welding Consumables Development, State of the Art, Science, and Reliability of Underwater Welding and Inspection Technology*. Houston, Tex.